

Analytical models for Cross-correlation signal in Time-Distance Helioseismology

R. Nigam, A. G. Kosovichev and P. H. Scherrer

W. W. Hansen Experimental Physics Laboratory, Stanford University, Stanford, USA

ABSTRACT

In time-distance helioseismology, the time signals (Doppler shifts) at two points on the solar surface, separated by a fixed angular distance are cross-correlated, and this leads to a wave packet signal. Accurately measuring the travel times of these wave packets is crucial for inferring the sub-surface properties in the Sun. The observed signal is quite noisy, and to improve the signal-to-noise ratio and make the cross-correlation more robust, the temporal oscillation signal is phase-speed filtered at the two points in order to select waves that travel a fixed horizontal distance. Hence a new formula to estimate the travel times is derived, in the presence of a phase speed filter, and it includes both the radial and horizontal component of the oscillation displacement signal. It generalizes the previously used Gabor wavelet that was derived without a phase speed filter and included only the radial component of the displacement. This is important since it will be consistent with the observed cross-correlation that is computed using a phase speed filter, and also it accounts for both the components of the displacement. The new formula depends on the location of the two points on the solar surface that are being cross correlated and accounts for the travel time shifts at different locations on the solar surface.

Subject headings: Sun: oscillations; Sun: phase speed; Sun: spherical harmonics

1. Introduction

Time-distance helioseismology (Duvall et al. 1993) constructs wave packets by cross-correlating time signals between any two points separated by a fixed horizontal angular distance on the solar surface. It then measures their travel time between the two points, by fitting a Gabor wavelet to the observed temporal cross-correlation (Kosovichev & Duvall 1997). This travel time is then inverted to study different properties (Kosovichev 1996; Zhao 2004) (e.g. sound speed perturbations, subsurface flows, meridional circulation) in the solar

interior that influence the wave packet, which cannot otherwise be studied by the global oscillations. The success in applying the technique depends on being able to design a phase speed filter of a certain width, that selects acoustic waves within a certain range of horizontal phase speeds, and this improves the signal-to-noise ratio (Duvall et al. 1997). Waves with the same horizontal phase speed travel the same horizontal distance on the solar surface, and therefore can be collectively used to probe the sub-surface features in the Sun, since they sample the same vertical depth inside the Sun. The filtering operation is carried out in the frequency domain, and it improves the signal-to-noise ratio by removing unwanted signals and waves that deviate a lot from the chosen phase speed, as these do not contribute to the cross-correlation, but instead can degrade it, and make the estimation of travel times inaccurate. The phase speed filter has a Gaussian shape centered at the desired phase speed, which is chosen to study waves traveling a particular horizontal distance.

Previous approaches to measuring the travel time between any two points was by fitting a Gabor wavelet (Kosovichev & Duvall 1997) to the measured cross correlation. This wavelet was derived by assuming that the amplitude of the solar oscillations has a Gaussian envelope in frequency of a certain width and peaked at a frequency where the power of the solar p-modes is concentrated, and moreover it considered only the radial component of the displacement. However, during data processing a phase speed filter is used. Also, the observed displacement on the solar surface has both radial and horizontal components. The horizontal component usually is ignored in the travel-time measurements. We show that it has a significant effect, particularly, for measurements far from the disk center and for moderate horizontal distances, contributing to systematic errors.

To remove the shortcomings, we derive a new analytical cross-correlation wavelet that incorporates the phase speed filter, and also includes both the radial and horizontal components of the Doppler velocity oscillation signal. This wavelet retains the structure of the Gabor wavelet, and is a function of the filter parameters: central phase speed and width, and also on the amplitude, phase and group travel times that depend on the oscillation properties and the dispersive nature of the solar medium. By including the horizontal component in the cross-correlation we also see a dependency on the location of the two points being cross-correlated, and moreover, the cross-correlation due to the horizontal component is a weighted sum of phase speed filtered Gabor wavelets, with the weights depending on the location of the cross-correlated points, the horizontal travel distance and the angular degree.

Comparing this with the original Gabor wavelet formula (Kosovichev & Duvall 1997) we can estimate how the phase-speed filter and the horizontal component shift the measured travel times. For the line depth and intensity observations, that only have a scalar (radial) component, in the weakly dispersive limit which is true for wave packets that probe the deeper

layers in the Sun and travel large horizontal distances on the solar surface, corresponding to small values of angular degree both formulae are similar. Hence, using the old Gabor wavelet in this regime should not effect the travel time measurements due to the phase speed filtering. On the other hand, wave packets constructed by cross-correlating time signals separated by a small horizontal distance, are distorted by the dispersive medium in the outer layers of the Sun, and, hence, the new formula should be used to account for the travel time shifts due to the phase-speed filtering procedure.

2. Cross-correlation of Phase Speed Filtered Signals

2.1. Scalar intensity and line depth filtered signal

In this section, we generalize the fitting formula of (Kosovichev & Duvall 1997) by including the phase-speed filtering. We first consider acoustic waves, that are observed by measuring either intensity fluctuations or line depth observations on the solar surface. They are represented as a sum of standing waves or normal modes at a point $\vec{r} = (r, \theta, \phi)$ in the solar interior and time t , and can be written as

$$h(r, \theta, \phi, t) = \sum_{n,l,m} a_{nlm} \psi_{nlm}(r, \theta, \phi) \exp \{i(\omega_{nlm}t - \alpha_{nlm})\} \quad (1)$$

where, $i = \sqrt{-1}$, and each normal mode is specified by a 3-tuple (l, m, n) of integer parameters, corresponding angular frequency ω_{nlm} , the mode amplitude a_{nlm} , the phase α_{nlm} and the spatial eigenfunction $\psi_{nlm}(r, \theta, \phi)$ as a function of the radial variable r and the angular variables (θ, ϕ) . The integer l denotes the degree and m the azimuthal order, $-l \leq m \leq l$, of the spherical harmonic

$$Y_l^m(\theta, \phi) = c_{lm} P_l^m(\cos \theta) \exp(im\phi), \quad (2)$$

which is a function of the co-latitude θ and longitude ϕ . Here, P_l^m is a Legendre function, and c_{lm} is a normalization constant. These describe the angular structure of the eigenfunctions. The third integer n of the 3-tuple (l, m, n) is called the radial order.

For a spherically symmetric Sun the eigenfunctions $\psi_{nlm}(r, \theta, \phi)$ can be separated into a radial function $\chi_{nl}(r)$ and an angular component $Y_l^m(\theta, \phi)$ (Unno et al. 1989). This representation is valid for example for the scalar intensity observations,

$$\psi_{nlm}(r, \theta, \phi) = \chi_{nl}(r) Y_l^m(\theta, \phi) \quad (3)$$

and also all modes with the same n and l have the same eigenfrequency ω_{nl} , regardless of the value of m . In reality the Sun is not spherically symmetric, that causes this degeneracy in m to be broken.

In time-distance helioseismology we measure the travel time of wave packets by forming a temporal cross-correlation between the oscillation signals at two locations separated by an angular distance on the solar surface $r = R$, where R is the solar radius. To model this we represent the solar oscillations on the solar surface as a linear superposition of normal modes, that are band-limited in angular frequency ω .

$$H(R, \theta, \phi, \omega) = 2\pi \sum_{n,l,m} a_{nlm} \chi_{nl}(R) Y_l^m(\theta, \phi) \exp(-i\alpha_{nlm}) \delta(\omega - \omega_{nlm}) \quad (4)$$

where $H(R, \theta, \phi, \omega)$ is the temporal Fourier transform (Bracewell 1999) of equation (1). We ignore mode damping and assume spherical symmetry, hence we can replace ω_{nlm} by ω_{nl} and invoke the band-limited nature of the solar spectrum, (Kosovichev & Duvall 1997; Giles 1999), by setting $a_{nlm} \chi_{nl}(R) = G_l(\omega)$, and we obtain from equation (4) the frequency band-limited signal $H_g(R, \theta, \phi, \omega) = H(R, \theta, \phi, \omega) G_l(\omega)$

$$H_g(R, \theta, \phi, \omega) = 2\pi \sum_{n,l,m} G_l(\omega) Y_l^m(\theta, \phi) \exp(-i\alpha_{nlm}) \delta(\omega - \omega_{nl}) \quad (5)$$

where, the Gaussian frequency function $G_l(\omega)$ captures the band-limited nature of the amplitude of the solar modes, and is given by

$$G_l(\omega) = b_l \exp\left(-\frac{(\omega - \omega_o)^2}{\delta\omega^2}\right) \quad (6)$$

The band-limited nature of the modes is controlled by the width $\delta\omega$, and a central frequency ω_o , where the power of the modes is peaked in the $\omega - l$ diagram. These two parameters change for different data sets, that probe different regions of the solar interior.

A phase speed filter is applied to the signal to select modes from the $\omega - l$ diagram for the purpose of constructing the cross-correlation wave packet. The phase speed filter is specified by a Gaussian centered around a phase speed V_{ph} and a width δV_{ph} as parameters, and is given by

$$F_p(V_p) = \exp\left(-\frac{(V_p - V_{ph})^2}{\delta V_{ph}^2}\right) \quad (7)$$

Where, the phase speed $V_p = \frac{\omega}{L}$, $L = \sqrt{l(l+1)} = k_h R$, k_h is the horizontal wave number. The role of the phase speed filter is to select waves with a small range of phase speeds, the range is specified by the width δV_{ph} . All these waves travel almost the same horizontal distance on the solar surface, and sample approximately the same vertical depth in the solar interior. Hence, it is crucial to select δV_{ph} appropriately so as to increase the signal-to-noise ratio in the cross-correlation function, and hence be able to better resolve the sub-surface structures in the Sun.

Due to the band-limited nature of the oscillation amplitudes, only values of L which are close to $L_o = \frac{\omega_o}{V_p}$ contribute to the sum in equation (5), and hence we Taylor expand L about the central frequency ω_o , upto first order:

$$L = L(\omega) = L[\omega_o + (\omega - \omega_o)] \approx L(\omega_o) + \frac{dL}{d\omega}(\omega - \omega_o) \quad (8)$$

The equation (8) can be written in terms of the angular group velocity $U_g = \frac{d\omega}{dL}$ and angular phase velocity $V_p = \frac{\omega}{L}$, evaluated at $\omega = \omega_o$, and using the fact $L(\omega_o) = \frac{\omega_o}{V_p}$, we have

$$L(\omega) \approx \frac{\omega}{U_g} + \left(\frac{1}{V_p} - \frac{1}{U_g} \right) \omega_o \quad (9)$$

Likewise, the phase velocity $V_p(L, \omega)$ can be expanded about the point (L_o, ω_o) in the $\omega - l$ diagram to yield

$$F_p(L, \omega) \approx \exp \left(- \frac{V_{ph}^2 \left(L - \frac{\omega}{V_{ph}} \right)^2}{\delta_f^2} \right) \quad (10)$$

where, $\delta_f = \frac{\omega_o \delta V_{ph}}{V_{ph}}$, and the filter width δV_{ph} is evaluated at (L_o, ω_o) , and is a constant.

Phase speed filtering takes place in the frequency domain and consists of multiplying the filter function $F_p(L, \omega)$ with the band-limited Fourier transformed signal $H_g(R, \theta, \phi, \omega)$ from equation (5).

$$H_{f_p}(R, \theta, \phi, \omega) = 2\pi \sum_{n,l,m} F_p(L, \omega) G_l(\omega) Y_l^m(\theta, \phi) \exp(-i\alpha_{nlm}) \delta(\omega - \omega_{nl}) \quad (11)$$

Equation (11) can be inverse Fourier transformed to yield the phase speed filtered temporal signal $h_{f_p}(R, \theta, \phi, t)$ at a point $\vec{R} = (R, \theta, \phi)$ on the solar surface. This signal now consists of a superposition of modes that lie in a region of the $\omega - l$ diagram, that is the intersection region of the frequency band-limited Gaussian envelope of the solar modes and the phase speed filter.

$$h_{f_p}(\vec{R}, t) = \sum_{n,l,m} F_p(L, \omega_{nl}) G_l(\omega_{nl}) Y_l^m(\theta, \phi) \exp(-i\alpha_{nlm}) \exp(i\omega_{nl}t) \quad (12)$$

The temporal cross-correlation function $\psi_{f_p}(\Delta, \tau)$ of the phase speed filtered signal $h_{f_p}(R, \theta, \phi, t)$ between two points A and B having coordinates $\vec{R}_1 = (R, \theta_1, \phi_1)$ and $\vec{R}_2 = (R, \theta_2, \phi_2)$ respectively on the solar surface with a fixed angular separation distance Δ , as a function of the time lag τ is

$$\psi_{f_p}(\Delta, \tau) = \frac{1}{T} \int_0^T h_{f_p}(\vec{R}_1, t) \bar{h}_{f_p}(\vec{R}_2, t + \tau) dt \quad (13)$$

where, \bar{h}_{f_p} is the complex conjugate of the phase speed filtered signal h_{f_p} , and T is the length of the time series.

Substituting the expression for $h_{f_p}(\vec{R}, t)$ from equation (12) into equation (13) one gets after applying the orthonormality of $\exp(-i\omega_{nl}t)$ in the temporal integral in equation (13)

$$\psi_{f_p}(\Delta, \tau) = \sum_{n,l} F_p^2(L, \omega_{nl}) G_l^2(\omega_{nl}) \exp(-i\omega_{nl}\tau) \sum_m \sum_{m'} Y_l^m(\theta_1, \phi_1) \bar{Y}_l^{m'}(\theta_2, \phi_2) \exp\{-i(\alpha_{nlm} - \alpha_{nlm'})\} \quad (14)$$

where, $\bar{Y}_l^{m'}(\theta_2, \phi_2)$ is the complex conjugate of $Y_l^{m'}(\theta_2, \phi_2)$. Since the phases are random, we assume that the term $\exp\{-i(\alpha_{nlm} - \alpha_{nlm'})\}$ in the double sum for m and m' is zero except when $m = m'$. In this case equation (14) becomes

$$\psi_{f_p}(\Delta, \tau) = \sum_{n,l} F_p^2(L, \omega_{nl}) G_l^2(\omega_{nl}) \exp(i\omega_{nl}\tau) \sum_m Y_l^m(\theta_1, \phi_1) \bar{Y}_l^m(\theta_2, \phi_2) \quad (15)$$

We can simplify equation (15) by applying the addition theorem of spherical harmonics (Jackson 1999)

$$\sum_m Y_l^m(\theta_1, \phi_1) \bar{Y}_l^m(\theta_2, \phi_2) = \frac{(2l+1)}{4\pi} P_l(\cos \Delta) \approx \frac{L}{2\pi} P_l(\cos \Delta) \quad (16)$$

where, P_l is the Legendre polynomial of order l , $L = \sqrt{l(l+1)} \approx l + \frac{1}{2}$ for large l (Christensen-Dalsgaard 2003), and Δ is the angular distance on the solar surface between the two points A (θ_1, ϕ_1) and B (θ_2, ϕ_2), and is (see Appendix A equations (49) and (50), Appendix D, Figure 6 and Appendix E, Figure 8)

$$\cos \Delta = \cos \theta_1 \cos \theta_2 + \sin \theta_1 \sin \theta_2 \cos(\phi_1 - \phi_2) \quad (17)$$

We can approximate for large l , small Δ , such that $L\Delta$ is large (Jackson 1999)

$$P_l(\cos \Delta) \approx J_0 \left[(2l+1) \sin \left(\frac{\Delta}{2} \right) \right] \approx \sqrt{\frac{2}{\pi L \Delta}} \cos \left(L\Delta - \frac{\pi}{4} \right) \quad (18)$$

where, J_0 is the Bessel function of the first kind. With this approximation from equation (18), the addition theorem in equation (16) becomes

$$\sum_m Y_l^m(\theta_1, \phi_1) \bar{Y}_l^m(\theta_2, \phi_2) = \frac{2}{\sqrt{\pi \Delta}} \frac{1}{2\pi} \sqrt{\frac{L}{2}} \cos \left(L\Delta - \frac{\pi}{4} \right) \quad (19)$$

Using equation (19), the equation (15) for the phase speed filtered cross-correlation becomes after taking the real part

$$\psi_{f_p}(\Delta, \tau) = \sum_{n,l} \frac{2}{\sqrt{\pi \Delta}} \frac{1}{2\pi} \sqrt{\frac{L}{2}} F_p^2(L, \omega_{nl}) G_l^2(\omega_{nl}) \cos(\omega_{nl}\tau) \cos \left(L\Delta - \frac{\pi}{4} \right) \quad (20)$$

The double sum in equation (20) can be reduced to a convenient sum of integrals if we regroup the modes so that the outer sum is over the phase speed $V_p = \frac{\omega_{nl}}{L}$, and the inner sum is over ω_{nl} (Kosovichev & Duvall 1997; Giles 1999). The expression for $\psi_{f_p}(\Delta, \tau)$ is an even function of τ , so we get an identical expression if we replace τ by $-\tau$ (negative time lag). The product of cosines in equation (20) can be transformed by using the trigonometric identity, and this results in

$$\psi_{f_p}(\Delta, \tau) = \sum_{V_p} \frac{1}{\sqrt{\pi\Delta}} \frac{1}{2\pi} \sqrt{\frac{L}{2}} \sum_{\omega_{nl}} F_p^2(L, \omega_{nl}) G_l^2(\omega_{nl}) \left[\cos\left(\omega_{nl}\tau - L\Delta + \frac{\pi}{4}\right) + \cos\left(\omega_{nl}\tau + L\Delta - \frac{\pi}{4}\right) \right] \quad (21)$$

In equation (21) we let $f_+(\omega_{nl}\tau) = \cos(\omega_{nl}\tau - L\Delta + \frac{\pi}{4})$ corresponding to the positive time lag τ and $f_-(\omega_{nl}\tau) = \cos(\omega_{nl}\tau + L\Delta - \frac{\pi}{4})$ corresponding to the negative time lag $-\tau$. Since cosine is an even function, it is seen that $f_-(\omega_{nl}\tau) = f_+(-\omega_{nl}\tau)$, hence we can drop $f_-(\omega_{nl}\tau)$ from equation (21), while extending the sum to negative values of ω_{nl} . We now substitute the expressions for the Gaussian envelope frequency function and the phase speed filter from equations (6) and (10) respectively into equation (21) and since ω_{nl} is a dummy variable in the inner sum, it is replaced by ω for notational convenience. Moreover, the inner sum over ω_{nl} can be replaced by an integral over ω , hence the discrete inner sum in equation (21) becomes

$$\psi_{f_p}(\Delta, \tau, V_p) = \int_{-\infty}^{\infty} d\omega \exp\left(-\frac{2V_{ph}^2 \left(L - \frac{\omega}{V_{ph}}\right)^2}{\delta_f^2}\right) \exp\left[-\frac{2}{\delta\omega^2}(\omega - \omega_o)^2\right] \cos\left(\omega\tau - L\Delta + \frac{\pi}{4}\right) \quad (22)$$

The integral in equation (22) is negligible for large frequencies hence there is very little error made in extending the frequency limit to ∞ and $-\infty$. Here, we choose the coefficient b_l for the Gaussian envelope function, such that

$$b_l^2 = 2\pi \sqrt{\frac{2}{L}} \quad (23)$$

In order to evaluate the integral in equation (22) we Taylor expand L , and using the linear dispersion relation from equation (9) we get

$$\left(L - \frac{\omega}{V_{ph}}\right) \approx \omega \left(\frac{1}{U_g} - \frac{1}{V_{ph}}\right) - \omega_o \left(\frac{1}{U_g} - \frac{1}{V_p}\right) \quad (24)$$

$$(\omega\tau - L\Delta) \approx \omega(\tau - \tau_g) - \omega_o(\tau_p - \tau_g) \quad (25)$$

where, the group travel time is defined as $\tau_g = \frac{\Delta}{U_g}$ and phase travel time $\tau_p = \frac{\Delta}{V_p}$.

Substituting equations (24) and (25) into the exponent of the phase speed filter and the argument of the cosine term respectively in equation (22), and carrying out the integral (Gradshteyn and Ryzhik 1994), which is bounded since the exponentials decay at both the limits of integration, with some algebra yields

$$\psi_{f_p}(\Delta, \tau, V_p) = A_{f_p}(\delta\omega, \delta_f, \tau, \tau_g, \tau_p) \cos \left\{ \left(\frac{R_g(\tau_g - \tau_p)}{\tau_{ph}} + \varepsilon^2 \right) \frac{\omega_o(\tau - \tau_g)}{R_g^2 + \varepsilon^2} + \omega_o(\tau_g - \tau_p) + \frac{\pi}{4} \right\} \quad (26)$$

Where, $R_g = \frac{\tau_g - \tau_{ph}}{\tau_{ph}}$ and $R_p = \frac{\tau_p - \tau_{ph}}{\tau_{ph}}$ are dimensionless quantities representing the relative deviation of the group and phase travel times respectively from the filter phase travel time, $\tau_{ph} = \frac{\Delta}{V_{ph}}$ and $\varepsilon^2 = \frac{\delta_f^2}{\delta\omega^2}$.

$$A_{f_p} = \sqrt{\frac{\pi}{2}} \frac{\delta\omega \varepsilon}{\sqrt{R_g^2 + \varepsilon^2}} \exp \left\{ -\frac{\delta\omega^2 \varepsilon^2}{8(R_g^2 + \varepsilon^2)} \left((\tau - \tau_g)^2 + \frac{16\omega_o^2 R_p^2}{\delta\omega^4 \varepsilon^2} \right) \right\} \quad (27)$$

The argument of the cosine term can be written as

$$\left(\frac{R_g(\tau_g - \tau_p)}{\tau_{ph}} + \varepsilon^2 \right) \frac{\omega_o(\tau - \tau_g)}{R_g^2 + \varepsilon^2} + \omega_o(\tau_g - \tau_p) = \omega_{f_p}(\tau - \tau_{f_p}) \quad (28)$$

where, the shifted frequency, $\omega_{f_p} = \omega_o(1 - R_{gp\varepsilon})$ and the shifted phase travel time due to the phase speed filter is

$$\tau_{f_p} = \tau_p - \frac{R_{gp\varepsilon}}{1 - R_{gp\varepsilon}} (R_g - R_p) \tau_{ph} \quad (29)$$

The dimensionless parameter $R_{gp\varepsilon} = \frac{R_g R_p}{R_g^2 + \varepsilon^2}$ is zero in the absence of phase speed filtering, which occurs when the filter width tends to infinity or in the non-dispersive limit when $R_g = R_p = 0$. Also from equation (29) we see a shift in the phase travel times due to the phase speed filtering, which tends to zero when $R_{gp\varepsilon}$ tends to zero. Also if we choose V_{ph} to be either V_p or U_g , then the effect of phase speed filtering can be removed since $R_g = R_p = 0$.

Summing equation (26) over phase velocities we get the final cross-correlation.

$$\psi_{f_p}(\Delta, \tau) = \sum_{V_p} \frac{1}{\sqrt{\pi\Delta}} \psi_{f_p}(\Delta, \tau, V_p) \quad (30)$$

In the non-dispersive limit when $R_g = R_p = 0$, that is $\tau_g = \tau_p = \tau_{ph}$, or in the limit of no phase speed filtering, large ε , equations (26) and (27) reduce to the original Gabor wavelet formula

$$\psi_{f_g}(\Delta, \tau, V_p) = \delta\omega \sqrt{\frac{\pi}{2}} \exp \left[-\frac{\delta\omega^2}{8} (\tau - \tau_g)^2 \right] \cos \left[\omega_o(\tau - \tau_p) + \frac{\pi}{4} \right] \quad (31)$$

In previous papers (Kosovichev & Duvall 1997; Giles 1999), the factor of $\frac{\pi}{4}$ has been absorbed in the phase travel time. By defining the phase travel time $\tau_p' = \tau_p - \frac{\pi}{4\omega_o}$, the Gabor wavelet in equation (31) reduces to the familiar form with the sinusoidal part being $\cos [\omega_o(\tau - \tau_p')]$.

We conclude that while the phase-speed filtering procedure does not change the functional form of the basic time-distance helioseismology fitting formula, it systematically shifts the travel times, if the filter parameter, V_{ph} , is different from the actual phase or group speeds for a given distance.

2.2. Effect of Line-of-Sight Doppler Velocity Measurements

We now consider the Doppler shift observations which are commonly used in helioseismology. The Doppler velocity depends on both the radial and horizontal components of the displacement. For simplicity, we take the axis of the spherical harmonics to be in the plane of the sky, orthogonal to the line of sight.

The displacement vector $\vec{d}(\vec{r}, t)$ at location $\vec{r} = (r, \theta, \phi)$ and time t is written for the spherically symmetric Sun as (Christensen-Dalsgaard 2002)

$$\vec{d}(\vec{r}, t) = \sum_{n,l,m} a_{nlm} \left\{ \xi_{nl}^r(r) Y_l^m(\theta, \phi) \hat{e}_r + \xi_{nl}^h(r) \left[\frac{\partial Y_l^m}{\partial \theta} \hat{e}_\theta + \frac{1}{\sin \theta} \frac{\partial Y_l^m}{\partial \phi} \hat{e}_\phi \right] \right\} \exp \{i(\omega_{nl}t - \alpha_{nlm})\} \quad (32)$$

where, $\xi_{nl}^r(r)$, $\xi_{nl}^h(r)$ are the radial and horizontal components of the displacement eigenfunctions respectively, and \hat{e}_r , \hat{e}_θ and \hat{e}_ϕ are unit vectors in r , θ and ϕ directions respectively (see Appendix A, Figure 5).

Thus, the observed Doppler signal on the solar surface is the projection of the displacement vector onto the line-of-sight direction. Without loss of generality we take the x-axis as the line-of-sight direction, hence the projection is just $\vec{d}(\vec{R}, t) \cdot \hat{e}_x$, where \hat{e}_x is the unit vector along the x-axis and is given by (see Appendix A, equation (46))

$$\hat{e}_x = \hat{e}_r \sin \theta \cos \phi + \hat{e}_\theta \cos \theta \cos \phi - \hat{e}_\phi \sin \phi \quad (33)$$

The Doppler signal on the solar surface is obtained by taking the dot product between $\vec{d}(\vec{R}, t)$ and the line of sight direction \hat{e}_x , and is therefore $d^x(\vec{R}, t) = \vec{d}(\vec{R}, t) \cdot \hat{e}_x = \sum_{n,l,m} d_{nlm}^x(\vec{R}, t)$. For a mode (l, m, n) it is

$$d_{nlm}^x(\vec{R}) = a_{nlm} \xi_{nl}^r(R) \left\{ Y_l^m(\theta, \phi) \sin \theta \cos \phi + \beta_{nl}(R) \left[\frac{\partial Y_l^m(\theta, \phi)}{\partial \theta} \cos \theta \cos \phi - \frac{\sin \phi}{\sin \theta} \frac{\partial Y_l^m(\theta, \phi)}{\partial \phi} \right] \right\} \quad (34)$$

where,

$$\beta_{nl}(R) = \frac{\xi_{nl}^h(R)}{\xi_{nl}^r(R)} = \frac{g(R)b_c}{R\omega_{nl}^2} \approx \frac{g(R)b_c}{R\omega_o^2} = \frac{b_c}{\sigma^2} \quad (35)$$

The ratio of horizontal to radial component $\beta_{nl}(R)$ shows dependence in frequency, and since the solar modes are band-limited in frequency, and peaked around ω_o , we replace the frequency ω_{nl} by a constant $\omega_o = 2\pi\nu_o$. Here, g is the acceleration due to gravity at the solar surface, σ is the dimensionless frequency and b_c is a factor that depends on the boundary condition used at the solar surface $r = R$. For the solar 5-min oscillations $\sigma^2 = \frac{R\omega_o^2}{g} \approx 1000$, and for the boundary condition that the Lagrangian pressure perturbation vanishes at the solar surface: at $r = R$, $\delta p = 0$, leads to $b_c = 1$, and this shows that at the solar surface the radial component dominates. For other types of boundary conditions the factor b_c may depend on L . If one selects waves with other frequencies, which are peaked around ν_1 instead of $\nu_o = 3.3$ mHz for the 5 minute oscillations, then the value of σ^2 at ν_1 can be easily calculated from $\sigma_1^2 \approx 1000 \left(\frac{\nu_1}{3.3}\right)^2$.

With the time dependence the Doppler signal is

$$d_{nlm}^x(\vec{R}, t) = d_{nlm}^x(\vec{R}) \exp \{i(\omega_{nl}t - \alpha_{nlm})\} \quad (36)$$

The cross-correlation $\psi_{f_p}^{d^x}(\vec{R}_1, \vec{R}_2, \tau)$ can be computed for the phase speed filtered Doppler signal $d_{f_p}^x(R, \theta, \phi, t) = \sum_{n,l,m} F_p(L, \omega_{nl}) d_{nlm}^x(\vec{R}, t)$ in a similar manner as for equation (12) and involves the product of the projected line of sight Doppler signals at the two locations A (θ_1, ϕ_1) and B (θ_2, ϕ_2) on the solar surface (See Figures 6 and 8). Here we have replaced $a_{nlm}\xi_{nl}^r(R)$ by the Gaussian frequency function $G_l(\omega)$, which models the amplitude of the solar modes.

$$\psi_{f_p}^{d^x}(\vec{R}_1, \vec{R}_2, \tau) = \frac{1}{T} \int_0^T d_{f_p}^x(\vec{R}_1, t) \bar{d}_{f_p}^x(\vec{R}_2, t + \tau) dt \quad (37)$$

In evaluating this cross-correlation we need the summation over m of the spherical harmonics and its derivatives, which are given in Appendix C.

Collecting all the sums over m we define the total sum (see Appendix C equations (95)-(98))

$$d_{nl}^x(\vec{R}_1, \vec{R}_2) = \sum_m d_{nlm}^x(\vec{R}_1) d_{nlm}^x(\vec{R}_2) = f_0 P_l(\cos \Delta) + f_1 \frac{dP_l(\cos \Delta)}{d\Delta} + f_2 \frac{d^2 P_l(\cos \Delta)}{d\Delta^2} \quad (38)$$

Substituting the expressions for $P_l(\cos \Delta)$ and its derivatives from Appendix B equations (56), (57) and (58), we obtain for large l , small Δ , such that $L\Delta$ is large

$$d_{nl}^x(\vec{R}_1, \vec{R}_2) = \sqrt{\frac{2}{\pi L \Delta}} \left[f_0 \cos \left(L\Delta - \frac{\pi}{4} \right) - l f_1 \sin \left(L\Delta - \frac{\pi}{4} \right) - l^2 f_2 \cos \left(L\Delta - \frac{\pi}{4} \right) \right] \quad (39)$$

where $L = \sqrt{l(l+1)}$ and $l = (L - \frac{1}{2})$. Equation (39) can be written as

$$d_{nl}^x(\vec{R}_1, \vec{R}_2) = \sqrt{\frac{2}{\pi L \Delta}} \left[A_l \cos\left(L\Delta - \frac{\pi}{4}\right) - B_l \sin\left(L\Delta - \frac{\pi}{4}\right) \right] = C_l \sqrt{\frac{2}{\pi L \Delta}} \cos\left(L\Delta - \frac{\pi}{4} + \zeta\right) \quad (40)$$

where, the phase factor $\zeta(\theta_1, \phi_1, \theta_2, \phi_2) = \tan^{-1}(B_l/A_l)$, $A_l = (f_0 - l^2 f_2)$, $B_l = l f_1$ and $C_l = \sqrt{A_l^2 + B_l^2}$. The value of L outside the trigonometric functions is evaluated at ω_o and is $L(\omega_o) = \frac{\omega_o}{V_p} = \frac{\omega_o \tau_p}{\Delta}$. The phase factor ζ in general is a function of frequency ω_{nl} , but since the solar oscillations are band-limited and their power is peaked at the frequency ω_o , ζ is evaluated at the central frequency ω_o . This also simplifies the evaluation of the integral, and a closed form expression can be derived. The phase shift ζ is measured in radians but can be converted to units of time by dividing by ω_o .

The cross-correlation is

$$\psi_{f_p}^{d^x}(\vec{R}_1, \vec{R}_2, \tau) = \sum_{n,l} F_p^2(L, \omega_{nl}) G_l^2(\omega_{nl}) \cos(\omega_{nl}\tau) d_{nl}^x(\vec{R}_1, \vec{R}_2) \quad (41)$$

Substituting the expression for $d_{nl}^x(\vec{R}_1, \vec{R}_2)$ from equation (40) into equation (41) and transforming the product of the cosines to a sum we obtain

$$\psi_{f_p}^{d^x}(\vec{R}_1, \vec{R}_2, \tau) = \sum_{V_p} \frac{2\pi C_l}{L\sqrt{\pi\Delta}} \frac{1}{2\pi} \sqrt{\frac{L}{2}} \sum_{\omega_{nl}} F_p^2(L, \omega_{nl}) G_l^2(\omega_{nl}) [f_{+h}(\omega_{nl}\tau, \zeta) + f_{-h}(\omega_{nl}\tau, \zeta)] \quad (42)$$

where, $f_{+h}(\omega_{nl}\tau, \zeta) = \cos(\omega_{nl}\tau - L\Delta + \frac{\pi}{4} - \zeta)$ and $f_{-h}(\omega_{nl}\tau, \zeta) = \cos(\omega_{nl}\tau + L\Delta - \frac{\pi}{4} + \zeta)$ correspond to positive and negative time lags respectively. Evaluating the inner sum in equation (42) in a similar manner as in equation (21) one obtains

$$\psi_{f_p}^{d^x}(\vec{R}_1, \vec{R}_2, \tau, V_p) = A_{f_p}(\delta\omega, \delta_f, \tau, \tau_g, \tau_p) \cos\left\{\omega_{f_p}(\tau - \tau_{f_{ph}}) + \frac{\pi}{4}\right\} \quad (43)$$

The shifted phase travel time $\tau_{f_{ph}}$ due to the horizontal component is therefore,

$$\tau_{f_{ph}} = \tau_{f_p} + \frac{\zeta}{\omega_{f_p}} \quad (44)$$

Summing equation (43) over phase velocities we get the final cross-correlation.

$$\psi_{f_p}^{d^x}(\vec{R}_1, \vec{R}_2, \tau) = \sum_{V_p} \frac{2\pi C_l}{L\sqrt{\pi\Delta}} \psi_{f_p}^{d^x}(\vec{R}_1, \vec{R}_2, \tau, V_p) \quad (45)$$

In deriving this equation we used the asymptotic formula for the Legendre functions, which allowed us to obtain the explicit expression for the phase shift. We verified by direct numerical calculations of the cross-covariance functions that this approximation is sufficiently accurate. A comparison of the analytical formula in equation (40) for $d_{nl}^x(\vec{R}_1, \vec{R}_2)$ with the direct numerical mode summation is shown in Figure 1. This approximation holds when the travel times are much greater than the oscillation period of five minutes, which is the case for typical time-distance measurements.

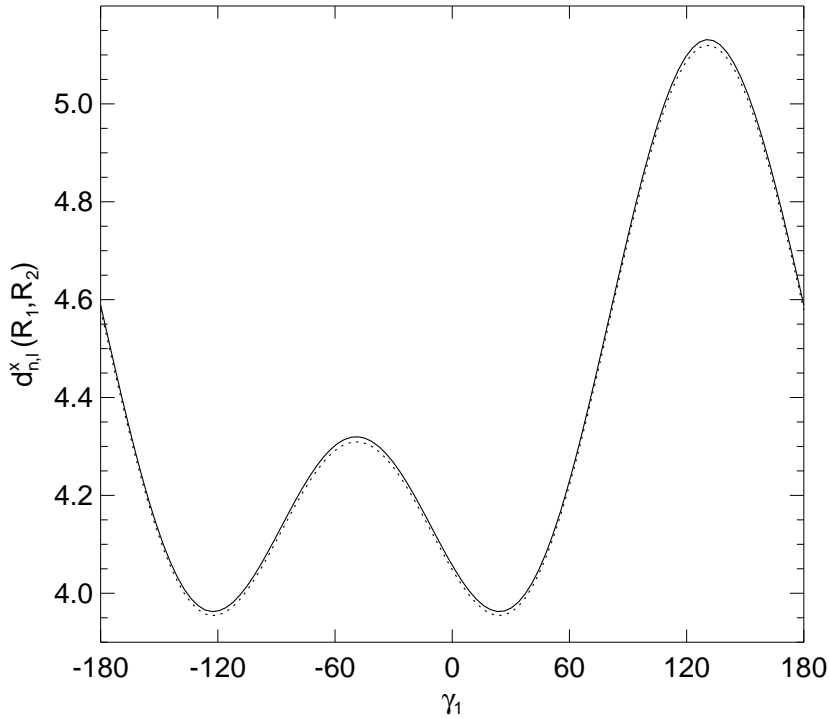


Fig. 1.— Comparison of function $d_{nl}^x(\vec{R}_1, \vec{R}_2)$, calculated numerically by direct mode summation given by the middle term in equation 38 (solid curve) and the analytical expression equation 40 (dotted curve). In this example, the central \vec{R}_1 point is located at $\theta_1 = 60^\circ$ and $\phi_1 = 30^\circ$, point \vec{R}_2 is located at a distance $\Delta = 8.4^\circ$ from \vec{R}_1 , and the angle, γ_1 between the directions from \vec{R}_1 to the North pole and point \vec{R}_2 varies from -180° to 180° , as illustrated in Figure 6, Appendix D.

From the equations (39) and (41) we observe that the cross-correlation of the Doppler line of sight velocity involving the horizontal component of the displacement is a weighted sum of the phase speed filtered Gabor wavelets, with the weights depending on the location $(\theta_1, \phi_1, \theta_2, \phi_2)$ of the two points being cross-correlated, and the angular degree l of the modes.

This weighted sum can be conveniently combined incorporating a phase factor into the cosine term.

From equation (44) we see a shift in phase travel times due to the horizontal component in addition to that introduced by the phase speed filtering. In Figure 2, we see a variation in the travel time shift due to the horizontal component as we move point B (see Appendix E, Figure 8) around the annulus by changing the angle γ_1 (see Appendix D, Figure 6), cross correlating with the fixed point A. Figure 3 illustrates the phase shift for the projection on the solar disk. The greatest phase shift changes happen for the outmost points in the direction from the disk center.

Averaging the travel time shift over the annular angle γ_1 , for different horizontal distances Δ and distances from disk center η , to simulate the observed mean travel times, we show in Figure 4 that this time shift increases (becomes more negative) as we go away from disk center and also for increasing horizontal distances. The shifts are quite appreciable, on the order of a few seconds, and have been observed in the real data from SOHO/MDI (Duvall 2003). At disk center C, (see Appendix E, Figure 7) which according to our convention is at $(y, z) = (0, 0)$, which is the origin of the YZ plane perpendicular to the line of sight direction \hat{e}_x . In polar coordinates the disk center is specified by $(\theta, \phi) = (\frac{\pi}{2}, 0)$, at which the horizontal component is zero in equation (34), and the radial component is maximum. We see from Figure 2, when point A is at disk center, the time shift is independent of γ_1 , moreover there will always be a small travel time shift for this case since point B is at a distance Δ from the disk center, and it has a non-zero horizontal component that when cross-correlated with the radial component of the signal at point A, which is at disk center, leads to a travel time shift.

3. Dispersive and Non-Dispersive Wave packets: Relation to the Gabor Wavelet without Phase Speed Filtering

A dispersive medium is where the phase velocity V_p is quite different from the group velocity U_g (Lighthill 1978; Whitham 1974). Due to this for a fixed distance Δ , the group and phase travel times are different. In the solar case the wave packets that travel short distances, probe the outer layers of the Sun, which are quite dispersive due to the presence of large gradients. Hence the wave packets got by the cross-correlation in equations (26) and (27) are distorted as they travel through the medium. Moreover, the approximations made by retaining only the first order terms in the Taylor expansion of the dispersion relation in equation (8) may be inadequate to completely model the physical effects associated with small distances, hence care must be exercised in interpreting the results got by using these

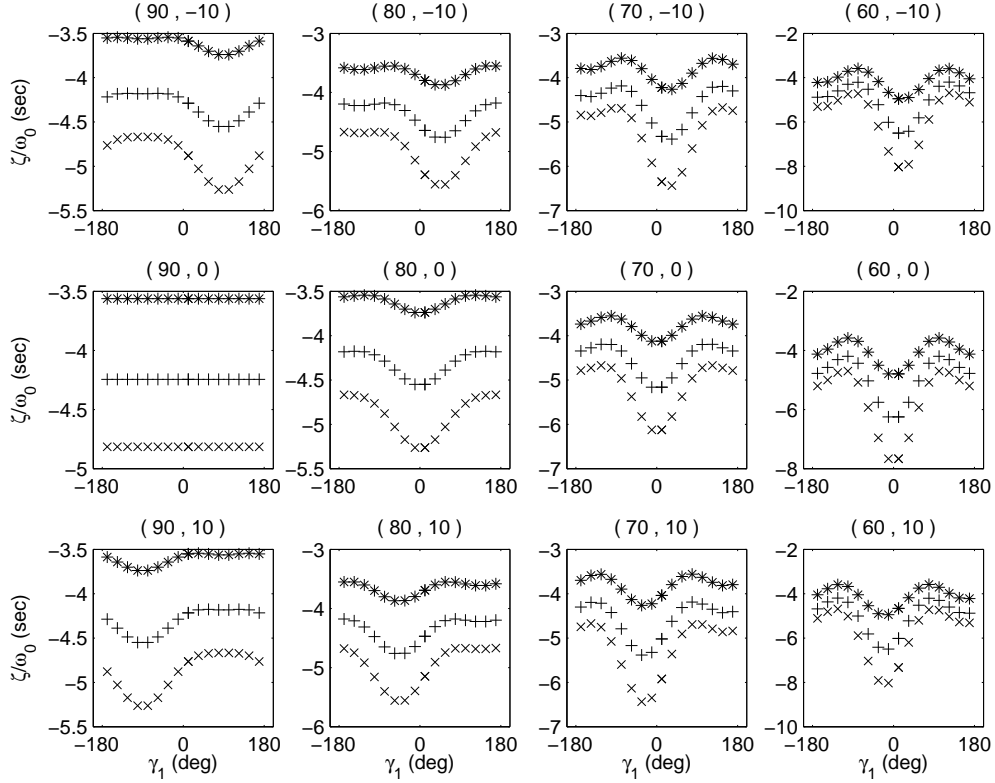


Fig. 2.— Phase shift (Y axis) $\frac{\zeta}{\omega_0}$ in seconds as a function of angle γ_1 (X axis) in degrees. The top most row corresponds to $\phi_1 = -10$ degrees, the next rows are in increments of 10 degrees. The left most column corresponds to $\theta_1 = 90$ degrees, the other columns are in decrements of 10 degrees. With this convention the left most plot of the second row corresponds to $(\theta_1, \phi_1) = (90^\circ, 0^\circ)$, for the annulus central point A, which is at disk center C. The star (*), plus (+) and cross (x) lines respectively in each plot correspond to $\Delta = 9.84, 15.36$ and 20.64 degrees, and $\tau_p = 58.89, 69.24$ and 77.01 minutes respectively. In this figure there is no shift due to phase speed filtering.

wavelets for small distances.

On the other hand, wave packets that travel large angular distances Δ , probe the deeper layers of the Sun, that are weakly dispersive, and hence undergo less distortion. It is quite interesting to note that the Gabor wavelet in equation (31), in the absence of the phase speed filter is got in the non-dispersive limit of equations (26) and (27) when $R_g = R_p = 0$, that is $\tau_g = \tau_p = \tau_{ph}$, for the intensity or line depth signal which has only the radial component. This is quite intuitive since in this limit there is no phase speed filtering, and $F_p(L, \omega) = 1$, hence the phase speed filtered signal in equation (11) reduces to the frequency band-limited signal

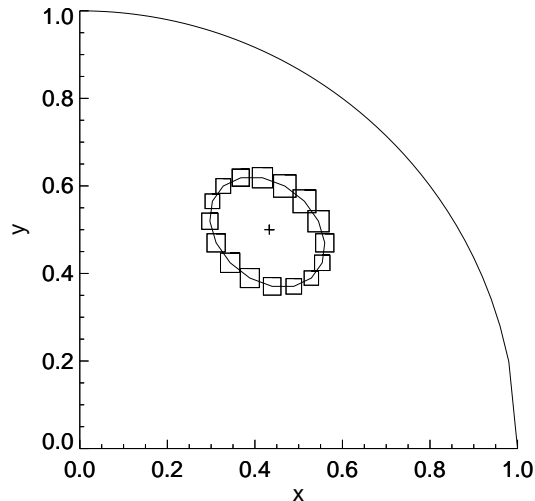


Fig. 3.— Illustration of the phase shift variations for a projection on the solar disk. The travel times are measured between the central point, located at $\theta_1 = 60$ degrees and $\phi_1 = 30$ degrees, and surrounding points at distance $\Delta = 8.4$ degrees and corresponding $\tau_p = 55.59$ minutes. The size of the symbols is proportional to the magnitude of the phase shifts which varies from -0.07 to -0.12 radians (corresponding to travel time shifts from -3.5 seconds to -5.5 seconds). In this Figure there is no phase speed filtering.

in equation (5). This is consisted both physically and mathematically. To form wave packets the medium need not be dispersive. Waves in a range of frequencies and wave lengths can interfere to form a wave packet. The wave packets that travel through a dispersive medium are distorted, where as those through a non-dispersive medium are not distorted, but retain their original shape.

The dimensionless quantities R_p and R_g measure the amount of deviation from non-dispersiveness. Hence to fit the observed temporal cross-correlation for the intensity or line depth signal where, R_g and R_p are small, there will be little error in using the Gabor wavelet of equation (31), since the new Gabor wavelet of equations (26) and (27) is very close to the old Gabor wavelet (Kosovichev & Duvall 1997; Giles 1999) in this non-dispersive or weakly dispersive limit for the line depth or scalar intensity signal that have only the radial component.

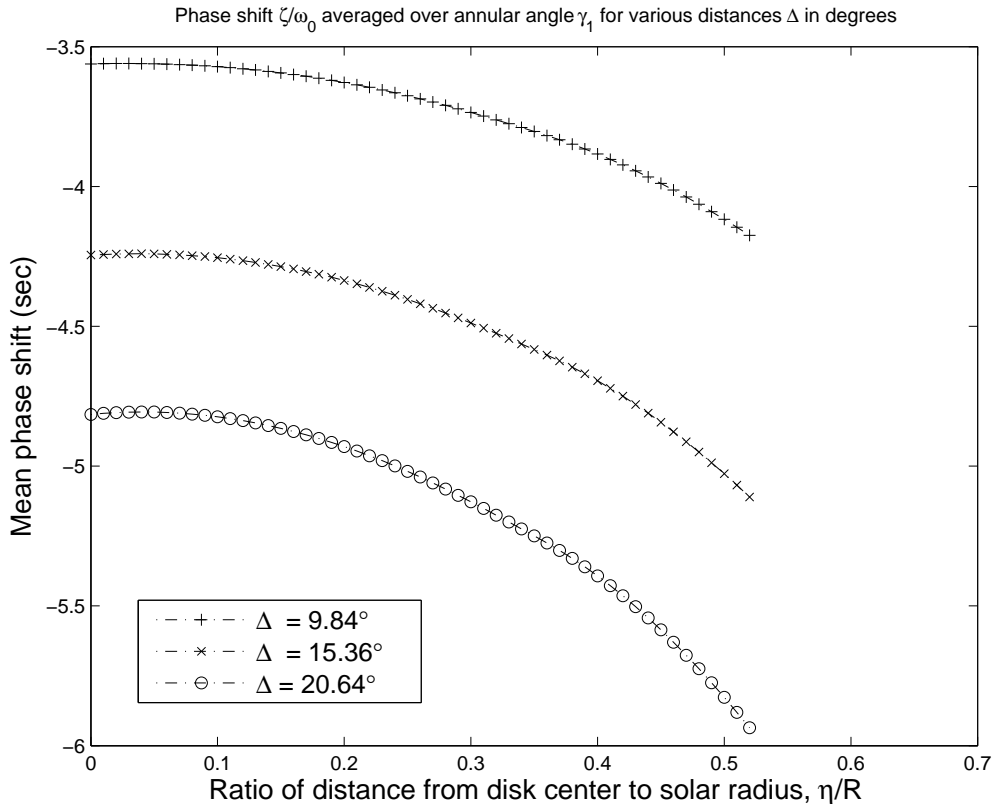


Fig. 4.— The mean phase shift in seconds (Y axis) got by averaging $\frac{\zeta}{\omega_0}$ over the annular angle γ_1 as a function of ratio with respect to solar radius of distance of the central point A from disc center C, $\frac{\eta}{R}$ (X axis). The star (*), plus (+) and cross (x) lines respectively correspond to $\Delta = 9.84$, 15.36 and 20.64 degrees, and $\tau_p = 58.89$, 69.24 and 77.01 minutes respectively. We observe a maximum travel time shift of about 6 seconds. This plot has no phase speed filtering, whose effect can be removed by choosing V_{ph} appropriately (see Sec.2.1).

4. Conclusion

In this paper we introduce a mathematical formalism to deal with the horizontal component of the displacement, which is used to derive a new formula to estimate travel times in time-distance helioseismology. It models the observed cross-correlation, by considering both the radial and horizontal components of the displacement, and also includes the phase speed filter on the frequency band-limited solar oscillations. The form of the Gabor wavelet is retained by the present formula, and in the non-dispersive limit for the line depth or intensity observations it reduces to the previously used Gabor wavelet that was derived without a phase speed filter, considering only the radial component. Including the horizontal compo-

ment, the cross-correlation is a weighted sum of phase speed filtered Gabor wavelets, with the weights depending on the angular position of the two points being cross-correlated, and the angular degree of the modes. Due to the phase speed filtering and inclusion of the horizontal component of the displacement, shifts in phase travel times are observed. In particular, the horizontal component induces a systematic shift in travel times, whose absolute value increases as we go away from disk center and also for large horizontal distances. This will in turn have implications in the inversions to study flows and the sub-surface properties in the Sun and also to formulate other local helioseismic approaches that involve the horizontal component.

5. Acknowledgments

This project was supported by the NASA MDI grant to Stanford University.

REFERENCES

- Bracewell, R., 2000, *The Fourier Transform and Its Applications*, 3rd edition (New York: McGraw-Hill)
- Christensen-Dalsgaard, J. 2002, *Rev. Mod. Phys.*, 74, 1073
- Christensen-Dalsgaard, J. 2003, *Lecture Notes on Stellar Oscillations*, 5th edition.
- Duvall, T. L., Jr., Jefferies, S. M., Harvey, J. W. & Pomerantz, M. A. 1993, *Nature*, 362, 430
- Duvall, T. L., Jr. et al. 1997, *Sol. Phys.*, 170, 63
- Duvall, T. L., Jr. 2003, *ESA SP-517: GONG+ 2002. Local and Global Helioseismology: the Present and Future*, 12, 259
- Giles, P. M. 1999, Ph.D. Thesis, Stanford University
- Gradshteyn, I. S. and Ryzhik, I. M. 1994, page 531, *Table of Integrals, Series, and Products* (5th edition), Academic Press, San Diego
- Jackson, J. D., 1999, *Classical Electrodynamics*, 3rd edition (New York: John Wiley & Sons)
- Jefferies, S.M., Osaki, Y., Shibahashi, H., Duvall, T.L., Jr., Harvey, J.W., & Pomerantz, M.A. 1994, *ApJ*, 434, 795

- Kosovichev, A. G. 1996, ApJ, 461, L55
- Kosovichev, A.G., Duvall, T.L., Jr. in SCORE-’96: Solar Convection and Oscillations and Their Relationship, ed. F.P. Pijpers et al., 1997 (Kluwer)
- Lighthill, M.J., 1978, Waves in Fluids (Cambridge: Cambridge University Press)
- Smart, W. M., 1977, Textbook on Spherical Astronomy, 6th edition (Cambridge: Cambridge University Press)
- Unno, W., Osaki, Y., Ando, H., & Shibahashi, H., 1989, Nonradial Oscillations of Stars (University of Tokyo Press, Tokyo)
- Whitham, G.B., 1974, Linear and Nonlinear Waves (New York: John Wiley & Sons)
- Winch, D. E. and Roberts, P. H. 1995, J. Austral Math Soc Ser B 37, 212
- Zhao, J. 2004 Ph.D. Thesis, Stanford University

6. Appendix A

We define the spherical coordinate system used in this paper (see Figure 5).

Consider fixed cartesian unit vectors $(\hat{e}_x, \hat{e}_y, \hat{e}_z)$ and the corresponding spherical unit vectors $(\hat{e}_r, \hat{e}_\theta, \hat{e}_\phi)$ that vary with the angles (θ, ϕ) . The equations relating these sets of unit vectors are

$$\hat{e}_x = \hat{e}_r \sin \theta \cos \phi + \hat{e}_\theta \cos \theta \cos \phi - \hat{e}_\phi \sin \phi \quad (46)$$

$$\hat{e}_y = \hat{e}_r \sin \theta \sin \phi + \hat{e}_\theta \cos \theta \sin \phi + \hat{e}_\phi \cos \phi \quad (47)$$

$$\hat{e}_z = \hat{e}_r \cos \theta - \hat{e}_\theta \sin \theta \quad (48)$$

Any point (x, y, z) in spherical coordinates (r, θ, ϕ) is $x = r \sin \theta \cos \phi$, $y = r \sin \theta \sin \phi$ and $z = r \cos \theta$. Consider two points A (θ_1, ϕ_1) and B (θ_2, ϕ_2) on the solar surface $r = R$ (see Figure 6, Appendix D), with coordinates $\vec{R}_1 = (x_1, y_1, z_1)$ and $\vec{R}_2 = (x_2, y_2, z_2)$, the

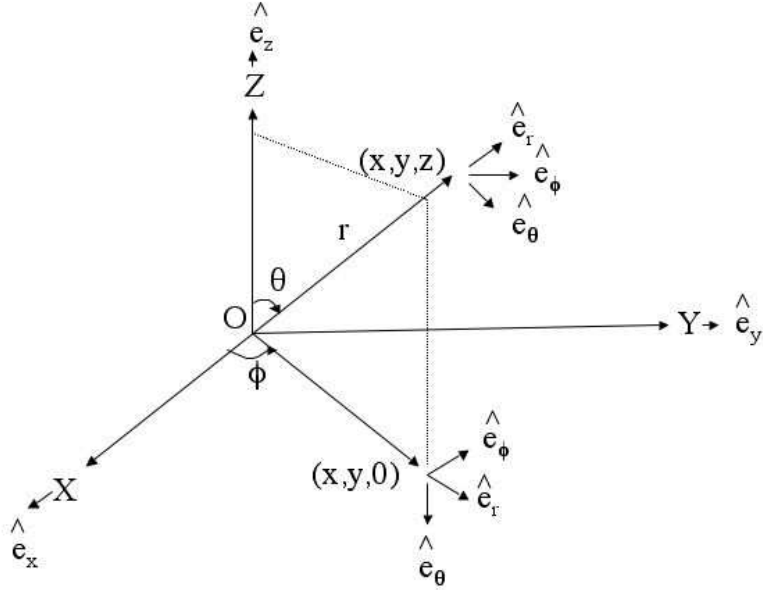


Fig. 5.— Spherical Coordinate System. The line of sight direction is along \hat{e}_x .

angular distance Δ between them can be calculated by taking the dot product of the unit vectors at these two locations and is given by

$$\cos \Delta = \frac{(\vec{R}_1 \cdot \vec{R}_2)}{R^2} = \frac{x_1 x_2 + y_1 y_2 + z_1 z_2}{R^2} \quad (49)$$

where, $(x_1, y_1, z_1) = (R \sin \theta_1 \cos \phi_1, R \sin \theta_1 \sin \phi_1, R \cos \theta_1)$ and $(x_2, y_2, z_2) = (R \sin \theta_2 \cos \phi_2, R \sin \theta_2 \sin \phi_2, R \cos \theta_2)$ (see Figure 6, Appendix D). Substituting this into equation (49) we obtain

$$\cos \Delta = \cos \theta_1 \cos \theta_2 + \sin \theta_1 \sin \theta_2 \cos(\phi_1 - \phi_2) \quad (50)$$

7. Appendix B

We derive various approximations for $P_l(\cos \Delta)$ and its derivatives for large l , small Δ and large $L\Delta$ following the approach of (Jackson 1999).

$$P_l(\cos \Delta) \approx J_0 \left[(2l + 1) \sin \left(\frac{\Delta}{2} \right) \right] \approx \sqrt{\frac{2}{\pi L \Delta}} \cos \left(L \Delta - \frac{\pi}{4} \right) \quad (51)$$

From the recursion relation (Jackson 1999),

$$\sin \Delta \frac{dP_l(\cos \Delta)}{d\Delta} - l \cos \Delta P_l(\cos \Delta) + l P_{l-1}(\cos \Delta) = 0 \quad (52)$$

For small Δ equation (52) becomes,

$$\Delta \frac{dP_l(\cos \Delta)}{d\Delta} - l P_l(\cos \Delta) + l P_{l-1}(\cos \Delta) = 0 \quad (53)$$

Differentiating equation (52) with respect to Δ gives

$$\sin \Delta \frac{d^2 P_l(\cos \Delta)}{d\Delta^2} - (l-1) \cos \Delta \frac{dP_l(\cos \Delta)}{d\Delta} + l \frac{dP_{l-1}(\cos \Delta)}{d\Delta} + l \sin \Delta P_l(\cos \Delta) = 0 \quad (54)$$

For small Δ and large l , equation (54) becomes,

$$\Delta \frac{d^2 P_l(\cos \Delta)}{d\Delta^2} - l \frac{dP_l(\cos \Delta)}{d\Delta} + l \frac{dP_{l-1}(\cos \Delta)}{d\Delta} + l \Delta P_l(\cos \Delta) = 0 \quad (55)$$

Now for small Δ , large l and large $L\Delta$ the various approximations are after using the recursion relations from equations (53) and (55)

$$P_l(\cos \Delta) \approx \sqrt{\frac{2}{\pi L \Delta}} \cos \left(L\Delta - \frac{\pi}{4} \right) \quad (56)$$

$$\frac{dP_l(\cos \Delta)}{d\Delta} \approx -l \sqrt{\frac{2}{\pi L \Delta}} \sin \left(L\Delta - \frac{\pi}{4} \right) \quad (57)$$

$$\frac{d^2 P_l(\cos \Delta)}{d\Delta^2} \approx -l^2 \sqrt{\frac{2}{\pi L \Delta}} \cos \left(L\Delta - \frac{\pi}{4} \right) \quad (58)$$

8. Appendix C

Using the addition theorem of the derivatives of spherical harmonics (Winch and Roberts 1995), we derive the expressions for the terms in equation (38).

The angular distance Δ is,

$$\cos \Delta = \cos \theta_1 \cos \theta_2 + \sin \theta_1 \sin \theta_2 \cos(\phi_1 - \phi_2) \quad (59)$$

Differentiating equation (59) with respect to θ_1 , θ_2 , ϕ_1 and ϕ_2 we obtain

$$\frac{\partial \Delta}{\partial \theta_1} = \frac{\sin \theta_1 \cos \theta_2 - \cos \theta_1 \sin \theta_2 \cos(\phi_1 - \phi_2)}{\sin \Delta} = \cos \gamma_1 \quad (60)$$

$$\frac{\partial \Delta}{\partial \theta_2} = \frac{\cos \theta_1 \sin \theta_2 - \sin \theta_1 \cos \theta_2 \cos(\phi_1 - \phi_2)}{\sin \Delta} = \cos \gamma_2 \quad (61)$$

$$\frac{\partial \Delta}{\partial \phi_1} = \frac{\sin \theta_1 \sin \theta_2 \sin(\phi_1 - \phi_2)}{\sin \Delta} = \sin \theta_1 \sin \gamma_1 \quad (62)$$

$$\frac{\partial \Delta}{\partial \phi_2} = -\frac{\sin \theta_1 \sin \theta_2 \sin(\phi_1 - \phi_2)}{\sin \Delta} = -\sin \theta_2 \sin \gamma_2 \quad (63)$$

The expressions in equations (60)-(63) can be equated to sine and cosine functions of γ_1 and γ_2 (Winch and Roberts 1995), which are shown in Figure 6, Appendix D using the results of spherical trigonometry (Smart 1977).

According to the addition theorem of spherical harmonics (Jackson 1999)

$$s_{nl}^{rr} = \sum_m Y_l^m(\theta_1, \phi_1) \bar{Y}_l^m(\theta_2, \phi_2) = \frac{(2l+1)}{4\pi} P_l(\cos \Delta) \quad (64)$$

For notational convenience we denote $N_l = \frac{(2l+1)}{4\pi}$. Differentiating equation (64) with respect to θ_2 and applying the chain rule leads to

$$s_{nl}^{r\theta} = \sum_m Y_l^m(\theta_1, \phi_1) \frac{\partial \bar{Y}_l^m(\theta_2, \phi_2)}{\partial \theta_2} = N_l \frac{dP_l(\cos \Delta)}{d\Delta} \frac{\partial \Delta}{\partial \theta_2} \quad (65)$$

Differentiating equation (64) with respect to ϕ_2 and applying the chain rule leads to

$$s_{nl}^{r\phi} = \sum_m Y_l^m(\theta_1, \phi_1) \frac{\partial \bar{Y}_l^m(\theta_2, \phi_2)}{\partial \phi_2} = N_l \frac{dP_l(\cos \Delta)}{d\Delta} \frac{\partial \Delta}{\partial \phi_2} \quad (66)$$

Differentiating equation (64) with respect to θ_1 and applying the chain rule leads to

$$s_{nl}^{\theta r} = \sum_m \frac{\partial Y_l^m(\theta_1, \phi_1)}{\partial \theta_1} Y_l^m(\theta_2, \phi_2) = N_l \frac{dP_l(\cos \Delta)}{d\Delta} \frac{\partial \Delta}{\partial \theta_1} \quad (67)$$

Differentiating equation (67) with respect to θ_2 and applying the product and chain rule gives

$$s_{nl}^{\theta\theta} = \sum_m \frac{\partial Y_l^m(\theta_1, \phi_1)}{\partial \theta_1} \frac{\partial \bar{Y}_l^m(\theta_2, \phi_2)}{\partial \theta_2} = N_l \left[\frac{\partial \Delta}{\partial \theta_1} \frac{\partial \Delta}{\partial \theta_2} \frac{d^2 P_l(\cos \Delta)}{d\Delta^2} + \frac{\partial}{\partial \theta_2} \left(\frac{\partial \Delta}{\partial \theta_1} \right) \frac{dP_l(\cos \Delta)}{d\Delta} \right] \quad (68)$$

Differentiating equation (67) with respect to ϕ_2 and applying the product and chain rule gives

$$s_{nl}^{\theta\phi} = \sum_m \frac{\partial Y_l^m(\theta_1, \phi_1)}{\partial \theta_1} \frac{\partial \bar{Y}_l^m(\theta_2, \phi_2)}{\partial \phi_2} = N_l \left[\frac{\partial \Delta}{\partial \theta_1} \frac{\partial \Delta}{\partial \phi_2} \frac{d^2 P_l(\cos \Delta)}{d\Delta^2} + \frac{\partial}{\partial \phi_2} \left(\frac{\partial \Delta}{\partial \theta_1} \right) \frac{dP_l(\cos \Delta)}{d\Delta} \right] \quad (69)$$

Differentiating equation (64) with respect to ϕ_1 and applying the chain rule leads to

$$s_{nl}^{\phi r} = \sum_m \frac{\partial Y_l^m(\theta_1, \phi_1)}{\partial \phi_1} \bar{Y}_1^m(\theta_2, \phi_2) = N_l \frac{dP_l(\cos \Delta)}{d\Delta} \frac{\partial \Delta}{\partial \phi_1} \quad (70)$$

Differentiating equation (70) with respect to θ_2 and applying the product and chain rule gives

$$s_{nl}^{\phi\theta} = \sum_m \frac{\partial Y_l^m(\theta_1, \phi_1)}{\partial \phi_1} \frac{\partial \bar{Y}_l^m(\theta_2, \phi_2)}{\partial \theta_2} = N_l \left[\frac{\partial \Delta}{\partial \phi_1} \frac{\partial \Delta}{\partial \theta_2} \frac{d^2 P_l(\cos \Delta)}{d\Delta^2} + \frac{\partial}{\partial \theta_2} \left(\frac{\partial \Delta}{\partial \phi_1} \right) \frac{dP_l(\cos \Delta)}{d\Delta} \right] \quad (71)$$

Differentiating equation (70) with respect to ϕ_2 and applying the product and chain rule gives

$$s_{nl}^{\phi\phi} = \sum_m \frac{\partial Y_l^m(\theta_1, \phi_1)}{\partial \phi_1} \frac{\partial \bar{Y}_l^m(\theta_2, \phi_2)}{\partial \phi_2} = N_l \left[\frac{\partial \Delta}{\partial \phi_1} \frac{\partial \Delta}{\partial \phi_2} \frac{d^2 P_l(\cos \Delta)}{d\Delta^2} + \frac{\partial}{\partial \phi_2} \left(\frac{\partial \Delta}{\partial \phi_1} \right) \frac{dP_l(\cos \Delta)}{d\Delta} \right] \quad (72)$$

Now using equations (34), (64)-(72) we obtain for the various terms in equation (38)

$$s_{nl}^1 = \sin \theta_1 \cos \phi_1 \sin \theta_2 \cos \phi_2 s_{nl}^{rr} = f_{10}^{rr}(\theta_1, \phi_1, \theta_2, \phi_2) P_l(\cos \Delta) \quad (73)$$

For notational convenience we denote the angular coordinates of points \vec{R}_1 and \vec{R}_2 by $\vec{a}_{12} = (\theta_1, \phi_1, \theta_2, \phi_2)$

$$s_{nl}^2 = \beta_{nl}(R) \sin \theta_1 \cos \phi_1 \cos \theta_2 \cos \phi_2 s_{nl}^{r\theta} = f_{21}^{r\theta}(\vec{a}_{12}) \frac{dP_l(\cos \Delta)}{d\Delta} \quad (74)$$

$$s_{nl}^3 = -\beta_{nl}(R) \sin \theta_1 \cos \phi_1 \frac{\sin \phi_2}{\sin \theta_2} s_{nl}^{r\phi} = f_{31}^{r\phi}(\vec{a}_{12}) \frac{dP_l(\cos \Delta)}{d\Delta} \quad (75)$$

$$s_{nl}^4 = \beta_{nl}(R) \cos \theta_1 \cos \phi_1 \sin \theta_2 \cos \phi_2 s_{nl}^{\theta r} = f_{41}^{\theta r}(\vec{a}_{12}) \frac{dP_l(\cos \Delta)}{d\Delta} \quad (76)$$

$$s_{nl}^5 = [\beta_{nl}(R)]^2 \cos \theta_1 \cos \phi_1 \cos \theta_2 \cos \phi_2 s_{nl}^{\theta\theta} = f_{52}^{\theta\theta}(\vec{a}_{12}) \frac{d^2 P_l(\cos \Delta)}{d\Delta^2} + f_{51}^{\theta\theta}(\vec{a}_{12}) \frac{dP_l(\cos \Delta)}{d\Delta} \quad (77)$$

$$s_{nl}^6 = -[\beta_{nl}(R)]^2 \cos \theta_1 \cos \phi_1 \frac{\sin \phi_2}{\sin \theta_2} s_{nl}^{\theta\phi} = f_{62}^{\theta\phi}(\vec{a}_{12}) \frac{d^2 P_l(\cos \Delta)}{d\Delta^2} + f_{61}^{\theta\phi}(\vec{a}_{12}) \frac{dP_l(\cos \Delta)}{d\Delta} \quad (78)$$

$$s_{nl}^7 = -\beta_{nl}(R) \frac{\sin \phi_1}{\sin \theta_1} \sin \theta_2 \cos \phi_2 s_{nl}^{\phi r} = f_{71}^{\phi r}(\vec{a}_{12}) \frac{dP_l(\cos \Delta)}{d\Delta} \quad (79)$$

$$s_{nl}^8 = -[\beta_{nl}(R)]^2 \frac{\sin \phi_1}{\sin \theta_1} \cos \theta_2 \cos \phi_2 s_{nl}^{\phi\theta} = f_{82}^{\phi\theta}(\vec{a}_{12}) \frac{d^2 P_l(\cos \Delta)}{d\Delta^2} + f_{81}^{\phi\theta}(\vec{a}_{12}) \frac{dP_l(\cos \Delta)}{d\Delta} \quad (80)$$

$$s_{nl}^9 = [\beta_{nl}(R)]^2 \frac{\sin \phi_1}{\sin \theta_1} \frac{\sin \phi_2}{\sin \theta_2} s_{nl}^{\phi\phi} = f_{92}^{\phi\phi}(\vec{a}_{12}) \frac{d^2 P_l(\cos \Delta)}{d\Delta^2} + f_{91}^{\phi\phi}(\vec{a}_{12}) \frac{dP_l(\cos \Delta)}{d\Delta} \quad (81)$$

Where we evaluate the derivatives of Δ with respect to θ_1 , θ_2 , ϕ_1 and ϕ_2 using equations (60)-(63) and the equations from (Winch and Roberts 1995), we obtain the following expressions

$$f_{10}^{rr}(\vec{a}_{12}) = N_l \sin \theta_1 \cos \phi_1 \sin \theta_2 \cos \phi_2 \quad (82)$$

$$f_{21}^{r\theta}(\vec{a}_{12}) = N_l \beta_{nl}(R) \sin \theta_1 \cos \phi_1 \cos \theta_2 \cos \phi_2 \cos \gamma_2 \quad (83)$$

$$f_{31}^{r\phi}(\vec{a}_{12}) = N_l \beta_{nl}(R) \sin \theta_1 \cos \phi_1 \sin \phi_2 \sin \gamma_2 \quad (84)$$

$$f_{41}^{\theta r}(\vec{a}_{12}) = N_l \beta_{nl}(R) \cos \theta_1 \cos \phi_1 \sin \theta_2 \cos \phi_2 \cos \gamma_1 \quad (85)$$

$$f_{51}^{\theta\theta}(\vec{a}_{12}) = -N_l [\beta_{nl}(R)]^2 \cos \theta_1 \cos \phi_1 \cos \theta_2 \cos \phi_2 \frac{\sin \gamma_1 \sin \gamma_2}{\sin \Delta} \quad (86)$$

$$f_{52}^{\theta\theta}(\vec{a}_{12}) = N_l [\beta_{nl}(R)]^2 \cos \theta_1 \cos \phi_1 \cos \theta_2 \cos \phi_2 \cos \gamma_1 \cos \gamma_2 \quad (87)$$

$$f_{61}^{\theta\phi}(\vec{a}_{12}) = N_l [\beta_{nl}(R)]^2 \cos \theta_1 \cos \phi_1 \sin \phi_2 \frac{\sin \gamma_1 \cos \gamma_2}{\sin \Delta} \quad (88)$$

$$f_{62}^{\theta\phi}(\vec{a}_{12}) = N_l [\beta_{nl}(R)]^2 \cos \theta_1 \cos \phi_1 \sin \phi_2 \cos \gamma_1 \sin \gamma_2 \quad (89)$$

$$f_{71}^{\phi r} = -N_l \beta_{nl}(R) \sin \phi_1 \sin \theta_2 \cos \phi_2 \sin \gamma_1 \quad (90)$$

$$f_{81}^{\phi\theta}(\vec{a}_{12}) = -N_l[\beta_{nl}(R)]^2 \sin \phi_1 \cos \theta_2 \cos \phi_2 \frac{\cos \gamma_1 \sin \gamma_2}{\sin \Delta} \quad (91)$$

$$f_{82}^{\phi\theta}(\vec{a}_{12}) = -N_l[\beta_{nl}(R)]^2 \sin \phi_1 \cos \theta_2 \cos \phi_2 \sin \gamma_1 \cos \gamma_2 \quad (92)$$

$$f_{91}^{\phi\phi}(\vec{a}_{12}) = N_l[\beta_{nl}(R)]^2 \sin \phi_1 \sin \phi_2 \frac{\cos \gamma_1 \cos \gamma_2}{\sin \Delta} \quad (93)$$

$$f_{92}^{\phi\phi}(\vec{a}_{12}) = -N_l[\beta_{nl}(R)]^2 \sin \phi_1 \sin \phi_2 \sin \gamma_1 \sin \gamma_2 \quad (94)$$

In computing the cross correlation in equation (41), we need to evaluate $d_{nl}^x(\vec{R}_1, \vec{R}_2)$ in equation (38) as

$$d_{nl}^x(\vec{R}_1, \vec{R}_2) = \sum_m d_{nlm}^x(\vec{R}_1) d_{nlm}^x(\vec{R}_2) = \sum_{i=1}^9 s_{nl}^i = f_0 P_l(\cos \Delta) + f_1 \frac{dP_l(\cos \Delta)}{d\Delta} + f_2 \frac{d^2 P_l(\cos \Delta)}{d\Delta^2} \quad (95)$$

where,

$$f_0(\vec{a}_{12}) = f_{10}^{rr} \quad (96)$$

$$f_1(\vec{a}_{12}) = f_{21}^{r\theta} + f_{31}^{r\phi} + f_{41}^{\theta r} + f_{51}^{\theta\theta} + f_{61}^{\theta\phi} + f_{71}^{\phi r} + f_{81}^{\phi\theta} + f_{91}^{\phi\phi} \quad (97)$$

$$f_2(\vec{a}_{12}) = f_{52}^{\theta\theta} + f_{62}^{\theta\phi} + f_{82}^{\phi\theta} + f_{92}^{\phi\phi} \quad (98)$$

9. Appendix D

In this appendix we derive the angular coordinates (θ_2, ϕ_2) of point B on the annulus, which is at a fixed annular angle γ_1 and a given angular distance Δ from the fixed point A with angular coordinates (θ_1, ϕ_1) at the center of the annulus. We use equations (59) and (60) from Appendix C to express the angular coordinates of B in terms of the fixed angles $(\theta_1, \phi_1, \gamma_1, \Delta)$. The geometry for the calculation is shown in Figure 6.

$$\cos \Delta = \cos \theta_1 \cos \theta_2 + \sin \theta_1 \sin \theta_2 \cos(\phi_1 - \phi_2) \quad (99)$$

$$\sin \Delta \cos \gamma_1 = \sin \theta_1 \cos \theta_2 - \cos \theta_1 \sin \theta_2 \cos(\phi_1 - \phi_2) \quad (100)$$

We now consider the case when the two points are close together, which is true for small distances Δ . They are related as $\theta_2 = \theta_1 + \delta\theta_1$ and $\phi_2 = \phi_1 + \delta\phi_1$, for small increments $\delta\theta_1$ and $\delta\phi_1$. The equations (99) and (100) can be expanded in terms of the increments, and using the standard trigonometric approximations for small angles $\sin \theta \approx \theta$ and $\cos \theta \approx 1 - \frac{\theta^2}{2}$ we obtain,

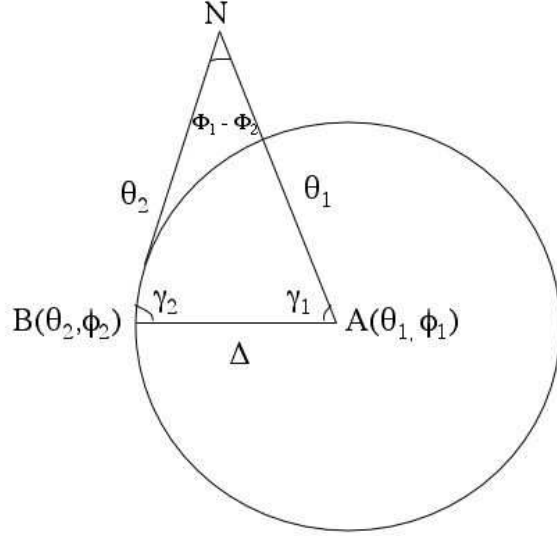


Fig. 6.— The Spherical Triangle showing Δ , which is the angular separation of the great circle arc between points A and B on the solar surface. Here, N is the North pole.

$$\delta\theta_1 = \Delta \left[1 - \frac{\sin^2 \gamma_1 \sin^2 \theta_1}{\sin^2 \theta_1 - \frac{\Delta}{2} \cos \gamma_1 \sin 2\theta_1} \right]^{\frac{1}{2}} \quad (101)$$

$$\delta\phi_1 = \frac{\Delta \sin \gamma_1}{\left[\sin^2 \theta_1 - \frac{\Delta}{2} \cos \gamma_1 \sin 2\theta_1 \right]^{\frac{1}{2}}} \quad (102)$$

For fixed Δ and γ_1 we use equations (101) and (102) to calculate (θ_2, ϕ_2) for small angular separation. For larger separations we can solve the linear equations (99) and (100) to calculate θ_2 , and equation (62) to compute ϕ_2 , and equations (61) and (63) to calculate $\cos \gamma_2$ and $\sin \gamma_2$ respectively.

10. Appendix E

In this appendix we consider the orthographic projection shown in Figure 7, where the points on the surface of the Sun are projected onto the YZ plane P, which is perpendicular

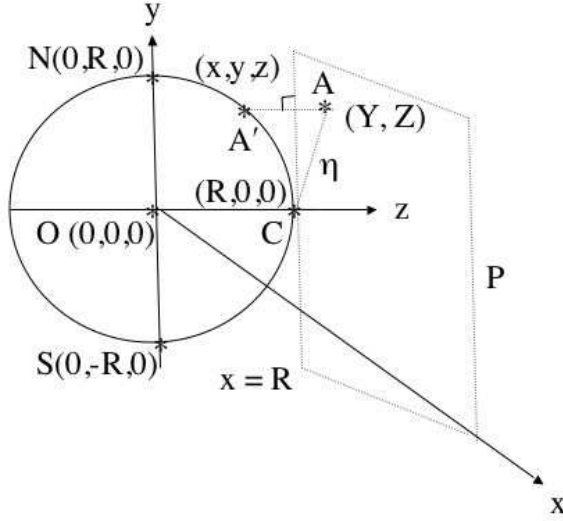


Fig. 7.— Orthographic projection. The point C is the disk center and η measures the distance from C to any projected point (Y,Z) on the orthographic plane P, which is at $x = R$. Any point A' on the solar surface is specified by (θ_1, ϕ_1) or the angle ϕ_1 and the distance η .

to the line of sight direction \hat{e}_x . The origin O is at the center of the Sun of radius R . We denote a point A' on the solar surface as (x, y, z) with axis xyz and as (Y, Z) the coordinate of the same point projected as A on the projection plane P with axis YZ . The x axis is perpendicular to the projection plane. The projection is oriented with north along $+y$ axis and east along the $+z$ axis. The projection is centered at co-latitude of 90° and longitude of 0° . With this convention, the north pole N has coordinates $(0, R, 0)$, the south pole S is $(0, -R, 0)$, and the point of tangency C between the sphere and the plane is $(R, 0, 0)$. The point C is also called the disk center. The projection plane is $x = R$. The coordinates of any point A' with co-latitude θ_1 and longitude ϕ_1 on the solar surface are

$$(x, y, z) = (R \sin \theta_1 \cos \phi_1, R \sin \theta_1 \sin \phi_1, R \cos \theta_1) \quad (103)$$

The equation of the sphere is $x^2 + y^2 + z^2 = R^2$. The coordinates of the same point on the plane are $(Y, Z) = (y, z)$. The point of tangency C between the sphere and the plane is the disk center and has coordinates $(Y, Z) = (0, 0)$ on the plane. Hence, the distance from the

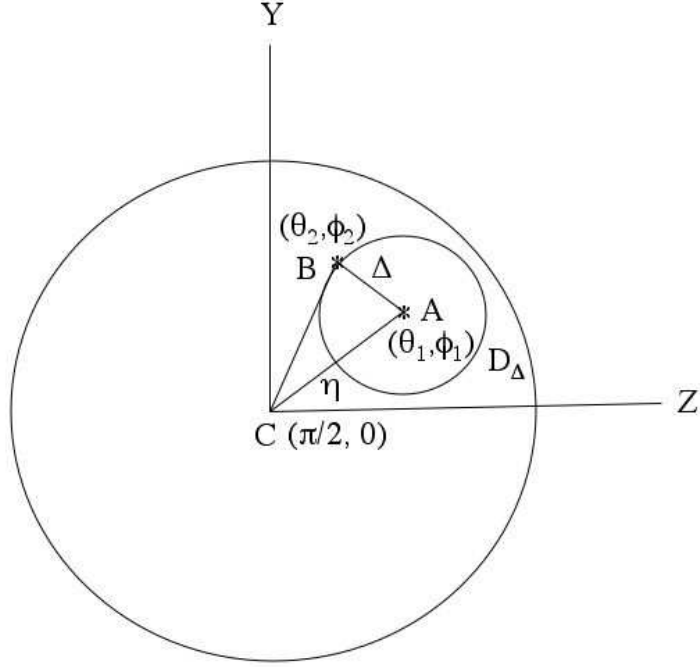


Fig. 8.— Projected Disc. This shows the annulus D_Δ of radius Δ around the point A (θ_1, ϕ_1) on the solar surface. The cross correlation is computed between the annulus center A and a point B (θ_2, ϕ_2) on the solar surface, that has an angular separation of Δ from A. The point A is at a distance η from the disk center C, $(\theta_c, \phi_c) = (\frac{\pi}{2}, 0)$.

disk center C $(0, 0)$ to any point A (Y, Z) on the plane P is denoted by η , which is fixed for each computation of the cross correlation. Any point A' on the solar surface and hence the corresponding projection A on the plane P can be specified by (θ_1, ϕ_1) or alternatively by the two parameters η and the angle ϕ_1 . In Figure 8, the center to annulus geometry is shown with the fixed center point A (θ_1, ϕ_1) , which is at a distance η from disk center C $(Y, Z) = (0, 0)$, and a point B (θ_2, ϕ_2) is on the annulus D_Δ of radius Δ .

$$\eta = (Y^2 + Z^2)^{\frac{1}{2}} = (y^2 + z^2)^{\frac{1}{2}} = (R^2 - x^2)^{\frac{1}{2}} = R(1 - \sin^2 \theta_1 \cos^2 \phi_1)^{\frac{1}{2}} \quad (104)$$

The angular coordinates of the disk center C, are $(\theta_c, \phi_c) = (\frac{\pi}{2}, 0)$. When the point A is at the disk center $(\theta_1, \phi_1) = (90^\circ, 0^\circ)$, and hence the distance $\eta = 0$. For fixed values of (Δ, γ_1) , together with the coordinates (θ_1, ϕ_1) of the annulus center A, we can compute the coordinates (θ_2, ϕ_2) of point B on the annulus by solving the linear system of equations (99) and (100) to get θ_2 and solving equation (62) to compute ϕ_2 .